Experimental Database for Surf-Riding and Broaching-to Quantification based on Captive Model Tests in Waves

Boris Horel [1*], Pierre-Emmanuel Guillerm [1], Jean-Marc Rousset [1] and Bertrand Alessandrini [1]

1. *Hydrodynamic, Energetics and Atmospheric Environment Laboratory (LHEEA), Ecole Centrale de Nantes, Nantes, France*

Abstract: With the aim of better understanding the phenomena of surf-riding and broaching for small service ships, a 6DOF numerical-experimental hybrid model based on semi-captive model tests in following waves has been created. Since a system based model is used, experiments are required in order to bring the hydrodynamic interactions between hull and water. In this paper, several semi-captive model tests in calm water and in following waves using a 1/10 scaled model of a trawler's hull will be presented. When navigating in astern seas, three modes of motion can be observed: the ship is overtaken by a wave, the ship is surfing a wave and the ship overtakes a wave.

Key words: Broaching, Surf-riding, Semi-captive model tests in waves

1. Introduction

Recent works concerning the Second Generation IMO Intact Stability Criteria showed that almost all of the world's fleet (fishing vessel, military ship, Ropax vessel...) is vulnerable to surf-riding and broaching (C. Wandji, P. Corrignan, 2012, [1]). Previous study brought out the instability boundary for an ONR tumblehome. It appears that surf-riding and broaching can be experienced by this military vessel for a wavelength to ship length ratio λ/L_{wl}=1.25 and a wave height to wavelength ratio H/λ=0.05 (S. Hosseini et al., 2010, [2]). With the aim of better quantifying these phenomena for small ships, semi-captive model tests in calm water and in following waves were conducted at the LHEEA towing tank, Nantes, France.

2. State of the Art

In 1999, N. Umeda et al. [3] confirmed with experiments that even a ship complying with the current IMO IS code can capsize as a result of broaching. It appears that surf-riding is regarded as a prerequisite of broaching.

In 2003, N. Umeda, H. Hashimoto and A. Matsuka [4] carried out captive model experiments on a 1/17.25 scaled model of a 135-gross-tonnage purse seiner in order to measure the restoring moment acting on the hull. The model was free in heave and pitch and was towed with a heel angle of 10° in following and quartering waves.

In 2004, H. Hashimoto et al. [5] proposed a new procedure for captive model experiments to obtain hydrodynamic forces. All experiments were conducted in calm water at various heel angles and Froude numbers corresponding to the case of an encounter frequency of 0. Some cases were chosen because they corresponded to the condition of a ship capsizing due to broaching in the ITTC benchmark test. For captive model tests, the 1/25 scaled model was equipped with a rudder but not a propeller, and was completely fixed in all directions.

In 2005, in order to validate their numerical code, Z. Ayaz, D. Vassalos and K.J. Spyrou [6] used results

*** Corresponding author:** Boris Horel, PhD student, research fields: hydrodynamic of ships and marine structures. E-mail: boris.horel@ec-nantes.fr

From model experiments on a 712 ton Japanese fishing vessel in extreme random seas. The captive model tests were conducted with different speeds, heading angle, sinkage, trim and in some cases with different wave steepness. They observed that the extremity of the conditions of captive model runs was defined within limits and strength of model that was used.

In 2008, R. Skejic and Odd M. Faltinsen [7] highlighted that no well-documented appropriate experimental results for manoeuvring of a ship in waves are available.

Still in 2008, since applicability of simulation models depends on the prediction accuracy of hydrodynamic forces, N. Umeda, A. Matsuda and H. Hashimoto [8] conducted captive model test experiments on a 1/48.94 scaled model of the ONR tumblehome vessel. The model was free in heave and pitch, and was attached with the towing carriage via a 4 component dynamometer. Heave and pitch were measured by a potentiometer and a gyroscope respectively. Experiments were then performed in waves at low encounter frequency. In these conditions, the model was towed with heel angles of 0, 10 and 20 degrees.

In 2009, S. Hosseini [9] carried out experiments on an ONR tumblehome in the INSEAN Basin and in the Osaka University towing tank. Resistance tests in calm water, static heel in calm water, static drift in calm water and static heel in following waves were performed to collect seakeeping and manoeuvring parameters for the Non-linear Dynamic Analysis (NDA) model of broaching.

In 2010, H. Hashimoto et al. [10] again performed captive model tests on the ONR tumblehome. They conducted resistance tests and propeller open water tests to estimate the resistance and the thrust of the subject ship. Circular motion tests (CMT) were also conducted at the seakeeping and manoeuvring basin of the NRIFE for combinations of drift angles and yaw rate. These CMTs were done without the propellers and the rudders. Linear and non-linear manoeuvring coefficients were obtained from the measured data by the least squared method. They pointed out that heel-induced hydrodynamic forces are important for broaching prediction so they measure the heel-induced hydrodynamic forces in calm water with forward velocity and several heel angles up to 70 degrees. To examine the roll restoring variation, they also conducted towing tank tests in following waves with different heel angles up to 70 degrees. In the experiment, the model was free in heave and pitch.

Inspired by the above state of the art experiments, we decided to design a purpose-built apparatus to perform semi-captive model experiments in waves. Resistance tests, static heel, static drift, pure sway and pure yaw both in calm water and in following waves were carried out.

3. Experimental Technique

3.1 Facilities

All the experiments were conducted in the towing tank of the LHEEA laboratory. The basin is 148 meters long, 5 meters wide and 3 meters deep. From low to medium speed, several model attitudes can be tested in one run, thereby improving the efficiency of the experimental campaign. The tank breadth makes it possible to perform pure sway tests with an amplitude of up to 0.6 meters. The carriage can reach a maximum speed of 8m/s.

3.2 Model

Fishing vessels are well known to suffer damage caused by the appearance of the broaching-to phenomenon. Marine investigation reports illustrate the extreme sea states and weather conditions of such a catastrophic event (Transportation Safety Board of Canada, 2009, [11]). It reveals that while a ship was navigating in astern seas, she lost her intact stability and capsized very quickly without the helmsman being able to influence the ship's heading. But these

Reports only provide qualitative aspects about the occurrence of this phenomenon.

The model is a 1/10 scaled model of a fishing vessel built as part of a project called OPTIPERF. This project was a collaborative project with HydrOcean and co-funded by the European Fisheries Fund (EFF). As shown in figure 1, this is an optimized-shape trawler, designed with a bifid bow to reduce drag due to wave field and hard chines to increase stability.

Fig. 1 - Hull shape of the model

The ship's features and the 1/10 scaled model features are given in table 1.

Table 1 Ship features

	Ship	*Model*
Length overall, L_{OA}	22.3 m	2.23 m
Waterline length, L_{wl}	21.3 m	2.13 m
Draft, T	3 m	0.3 m
Displacement, ∇	164 ton	160 kg
Longitudinal position of centre of gravity, x_{CG}	11.2 m	1.12 m
Roll moment of inertia, I_{Gx}	880 t.m²	8.8 kg.m²
Pitch moment of inertia, I_{Gy}	4700 t.m²	47 kg.m²
Yaw moment of inertia, I_{Gz}	4800 t.m²	48 kg.m²

The model was equipped with propeller and rudder in order to measure the influence of appendages on resultant forces acting on the hull.

When performing tests, the propeller revolution rate was set to a constant value.

Since the friction forces at full scale are smaller than at model scale, the full scale self-propulsion point was chosen instead of the model scale self-propulsion point to avoid the overestimation of the viscosity effect on the rudder.

An important part of trying to understand dynamical phenomena and their simulation is to accurately adjust the moments of inertia values. Indeed, when performing tests in waves the model was free in heave, pitch and roll, thus the recorded forces, moments and attitude are highly influenced by the roll moment of inertia, the pitch moment of inertia and loading conditions in calm water *GM*.

The moments of inertia were adjusted in the air using the compound pendulum theory. Then, by measuring the period T_M of the model oscillations, the following formulation gives the value of the pitch moment of inertia I_{Gy} expressed at the centre of gravity:

$$I_{Gy} = \nabla g \left\| \overrightarrow{OG} \right\| \left(\frac{T_M}{2\pi} \right)^2 - \nabla \left\| \overrightarrow{OG} \right\|^2 \qquad (1)$$

When using this kind of adjustment, the higher the moment of inertia, the lower the uncertainty is.

3.3 Instrumentation

Because the broaching-to phenomenon is well known to be an abrupt change of the kinematic in the horizontal plane (K.J. Spyrou, 2000, [12]), we decided to design a measurement system inspired by a planar motion mechanism (PMM), making it possible to measure forces and moments acting on the ship while she was towed in following waves

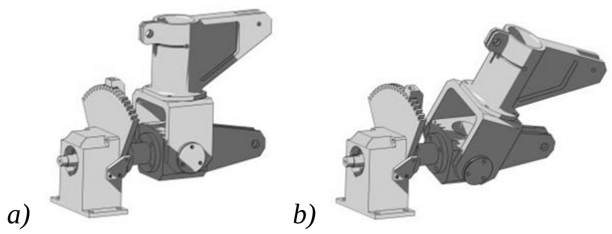

Fig. 2 - Articulation in upright position *a)*, articulation in a randomly adjusted position *b)*

As shown above in figure 2, new articulations have been designed in order to adjust the roll and pitch angles. According to the kind of test to be performed, roll, pitch and heave can be independently adjusted. Then, several combinations can be tested for roll (free or fixed), pitch (free or fixed) and heave (free or fixed).

a)

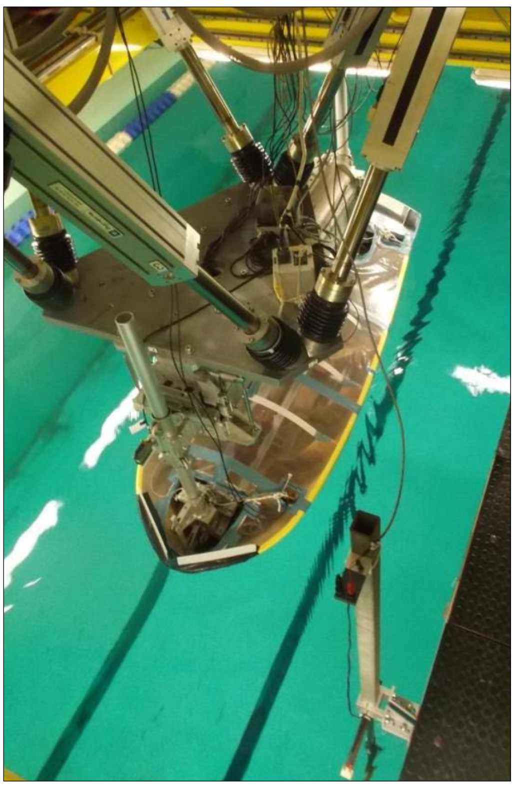

b)

Fig. 3 - *a)* Inertial setting and the mounting of the model on the dynamometer; *b)* Configuration with the *6DOF* hexapod

As shown in figure 3, the model was connected to a 6-component dynamometer by two vertical columns making possible the heave motion. The whole apparatus was mounted on a 6 degrees of freedom hexapod.

The main advantage of such a system is to make possible resistance tests, drift tests and harmonic tests (pure sway and pure yaw) both in calm water and in waves.

With the aim of studying their influence on forces and moments, following attitude parameters were measured: roll angle, pitch angle, heave motion. In parallel, surge force, sway force, heave force (if no heave motion), roll moment, pitch moment, yaw moment, thrust and torque on the propeller, lift and drag on the rudder were measured. Other parameters such as carriage velocity, motor angular rate and wave elevation were also measured at the ship's bow.

In our mathematical model, the rudder forces are modelled as external forces and there are no hydrodynamic derivatives relative to the rudder that will be defined (B. Horel et al., 2013, [13]). Thus we decided to create a 3D-printed rudder using a *NACA0015* profile whose lift and drag coefficients are knowledgeable in the literature.

4. Mathematical Model

The objective of the experiments is to express hydrodynamic derivative values of a manoeuvring model by post-processing the recorded signals. Inspired by the manoeuvring model of D. Obreja et al. [14], the mathematical model that has been established to model the broaching phenomenon is a *6DOF* model. However, towing tank tests were only used to create a *4 DOF* force model whose surge X_0, sway Y_0, roll K_0 and yaw N_0 components in calm water are defined using Taylor's series as follow:

$$X_0 = X_{\dot{u}}\dot{u} + X_u u + \frac{1}{2}X_{uu}u^2 + \frac{1}{6}X_{uuu}u^3 + X_{\dot{v}}\dot{v} + X_v v + \frac{1}{2}X_{vv}v|v| + X_{uv}uv + X_{\dot{r}}\dot{r} + X_r r + \frac{1}{2}X_{rr}r|r| + X_{ur}ur \quad (2)$$

$$Y_0 = Y_{\dot{v}}\dot{v} + Y_v v + \frac{1}{2}Y_{vv}v|v| + \frac{1}{6}Y_{vvv}v^3 + Y_{uv}uv + Y_{\dot{r}}\dot{r} + Y_r r + \frac{1}{2}Y_{rr}r|r| + Y_{ur}ur \quad (3)$$

$$K_0 = K_{\dot{v}}\dot{v} + Y_v v + \frac{1}{2}K_{vv}v|v| + K_{uv}uv + K_{\dot{r}}\dot{r} + K_r r + \frac{1}{2}K_{rr}r|r| + K_{ur}ur \quad (4)$$

$$N_0 = N_{\dot{v}}\dot{v} + N_v v + \frac{1}{2}N_{vv}v|v| + N_{uv}uv + N_{\dot{r}}\dot{r} + N_r r + \frac{1}{2}N_{rr}r|r| + N_{ur}ur \quad (5)$$

Those previous equations are the general expressions for forces acting on the hull in calm water. A significant change occurs when the vessel is navigating in following waves, so an encounter frequency dependent wave function is added to previous equations. The latter can be expressed as function of encounter frequency ω_e, relative position compared to the wave trough ξ_G/λ, wavelength to ship length ratio λ/L_{wl} and wave height to wavelength ratio H/λ.

5. Analysis Procedure

Both in calm water and while surfing in waves at zero encounter frequency, three main kinds of tests were performed and each of them has to be analyzed using one of the procedures described below.

5.1 Stationary Motion

Following stationary tests were performed for several trim and heel angles:

- Straight towing
- Straight towing with rudder deflection

X_u , X_{uu} and X_{uuu} are deduced from straight towing tests.

- Oblique towing
- Oblique towing with rudder deflection

X_v , X_{vv} , X_{uv} , Y_v , Y_{vv} , Y_{vvv} ,Y_{uv} , K_v , K_{vv} , K_{uv} ,N_v , N_{vv} and N_{uv} are calculated from oblique towing tests.

The analysis of these results is based on the averaging of the recorded signals. Samples are analysed for a minimum period of 15 seconds. The raw values are given in Volts at the reduction point of the dynamometer located around 1 meter above the model centre of gravity. Thus, once the dimensional values are calculated, it is necessary to express them in the ship coordinate system whose origin is at the centre of gravity instead of in the dynamometer coordinate system.

5.2 Harmonic Motion

Then, the following harmonic tests were also carried out for several trim and heel angles:

- Pure sway

$X_{\dot{v}}$, $Y_{\dot{v}}$, $K_{\dot{v}}$ and $N_{\dot{v}}$ are deduced from pure sway tests.

- Pure yaw

$X_{\dot{r}}$, X_r , X_{rr} , X_{ur} , $Y_{\dot{r}}$, Y_r , Y_{rr} , Y_{ur} , $K_{\dot{r}}$, K_r , K_{rr} , K_{ur} , $N_{\dot{r}}$, N_r , N_{rr} , N_{ur} are calculated from pure yaw tests.

For those tests, depending on the tank length, a minimum number of periods is needed to analyze the signals. Four sets of amplitudes *A* and periods *T* were tested: *A*=0.2m *T*=6s; *A*=0.2m *T*=9s; *A*=0.3m *T*=6s and *A*=0.3m *T*=9s.

Parts of the measured signal in-phase with acceleration and in-phase with velocity are determined using Fourier's series.

5.3 Accelerated Motion

In order to determine the added mass in surge, the following accelerated tests were performed only in calm water for several trim angles:

- Straight towing

$X_{\dot{u}}$ is deduced from straight towing tests.

This hydrodynamic derivative can only be determined once the hydrodynamic coefficients from straight towing tests are determined. In fact, the theoretical signal without acceleration is deducted from the measured signal. The remaining part is only due to acceleration and makes possible to compute $X_{\dot{u}}$.

6. Results

In this part of the paper, results in calm water and in waves will be presented. Experimental results are low pass filtered before being analyzed.

6.1 Calm Water

In the study of forces acting on the hull while performing straight towing at zero trim angle, zero heel angle and zero drift angle, figure 4 shows the comparison between measured values (blue dots) and the model. Hydrodynamic coefficients have been calculated using a polynomial regression method.

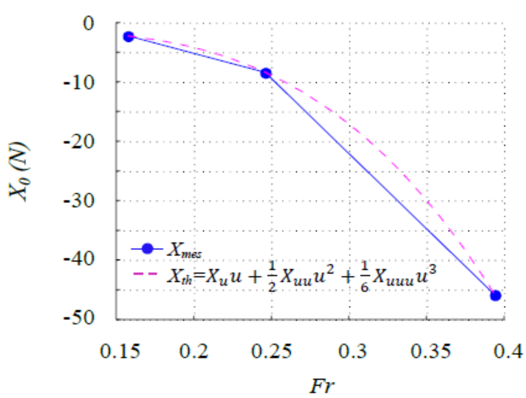

Fig. 4 - Resistance test: influence of the Froude number on the measured surge force

Then the post processing of oblique towing tests shows the influence of the sway velocity on the measured forces. From these tests, it is also possible to compute the coupling term between surge velocity u and sway velocity v. Indeed, previous studies reveal that coupling terms are relevant when trying to quantify the broaching-to phenomenon.

Oblique towing with drift angle β and constant carriage speed U_c means that sway velocity is not equal to zero, then:

$$u = U_c \cos\beta \tag{6}$$

$$v = -U_c \sin\beta \tag{7}$$

Figure 5 shows the mathematical model results compared to the experimental values. A good accordance is found when trying to fit the curves with non-linear terms. The graphs legend is as follows:

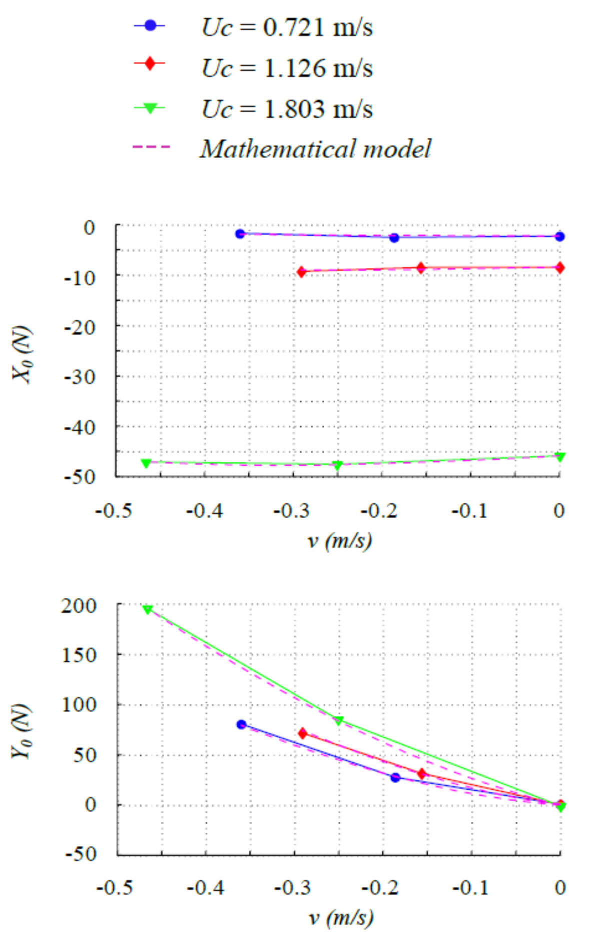

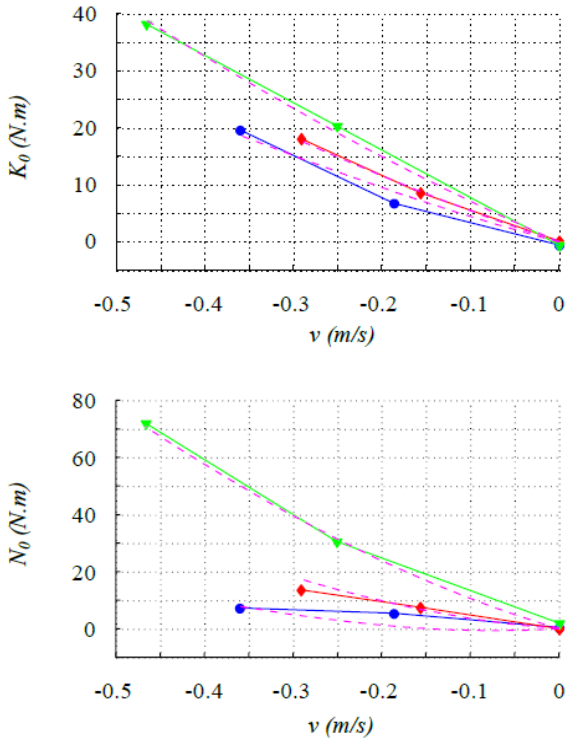

Fig. 5 - Oblique test: comparison between experimental results and mathematical model; surge force X_0, sway force Y_0, roll restoring moment K_0 and yaw moment N_0

Because our *6 DOF* model is a seakeeping and manoeuvrability coupled model, and also because the validation of the force model on the rudder is needed, we performed drift tests with rudder deflection. Influence of rudder angle δ on ship resistance for Uc=1.126m/s is shown in figure 6 below:

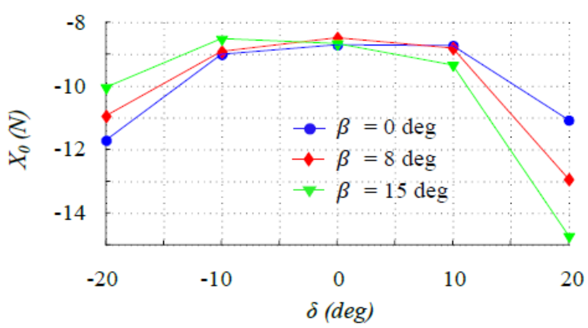

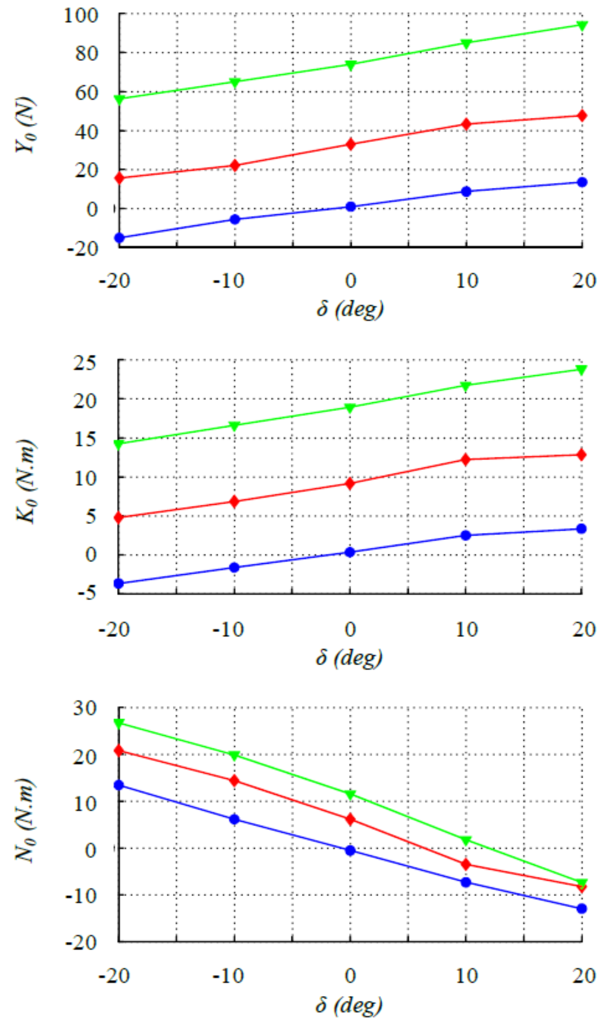

Fig. 6 - Drift tests with rudder deflection: Experimental results

The full determination of the model's hydrodynamic derivatives requires performing harmonic tests. Motions were generated using a *6 DOF* hexapod. Rotation in yaw was done at the centre of gravity around the vertical axis. Dynamometer's mass and inertia were first determined from pure sway and pure yaw tests without model. Then, deducing dynamometer effects from the recorded signal, figure 7 shows for A=0.3m and T=6s that for pure yaw tests, there is still a good agreement to be found between our model in calm water and experimental results.

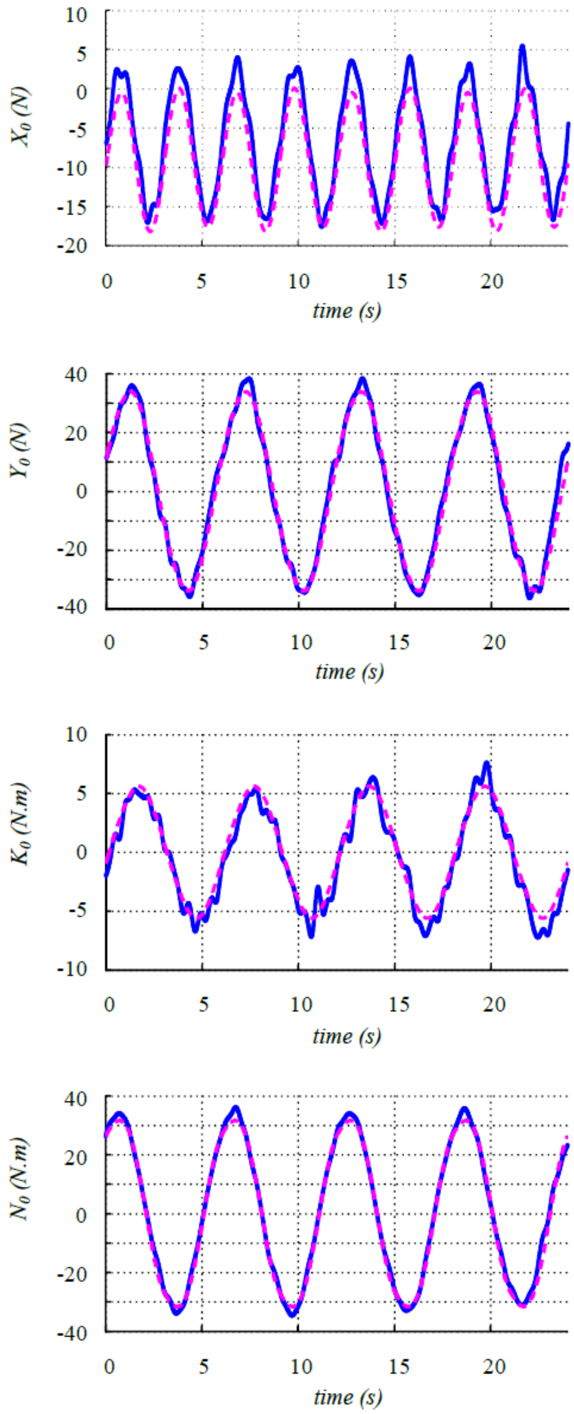

Fig. 7 - Pure yaw test: comparison between experimental results (blue line) and mathematical model (magenta dashed line)

This model in calm water is of importance because it is the basis of the mathematical model in waves.

6.2 Following Waves

Figure 8 shows a surf-riding test, while the centre of gravity of the model is located on a wave crest.

Fig. 8 - Surf-riding test while navigating on a wave crest

As previously mentioned, while surfing a wave, the experimental data have shown that forces acting on the hull can be derived from forces in calm water adding a function depending on wave parameters and encounter frequency. For instance, a first model has been developed in surge direction. The total resistance X can be expressed in terms of surge force in calm water X_0 as follow:

$$X = X_0 + \left[X_{Hc}\frac{H}{\lambda} + \frac{1}{2}X_{HHc}\left(\frac{H}{\lambda}\right)^2 + X_{\lambda c}\frac{\lambda}{L_{wl}} + \frac{1}{2}X_{\lambda\lambda c}\left(\frac{\lambda}{L_{wl}}\right)^2 + f_A(\omega_e)\right]\cos\left(2\pi\frac{\xi_G}{\lambda} + \frac{1}{2}\pi\left(20\frac{H}{\lambda} - 1\right) - f_\varphi(\omega_e)\right) + X_\lambda\frac{\lambda}{L_{wl}} + \frac{1}{2}X_{\lambda\lambda}\left(\frac{\lambda}{L_{wl}}\right)^2 - f_{offset}(\omega_e) \qquad (8)$$

X_{Hc} , X_{HHc} , $X_{\lambda c}$, $X_{\lambda\lambda c}$, X_λ , and $X_{\lambda\lambda}$ are hydrodynamic derivatives.

Previous experimental tests have been done at low encounter frequency, but rarely at exact zero encounter frequency (H. Hashimoto et al., 2004 [4]). This has been possible by synchronizing the carriage start with the wave maker start. Using the dispersion relationship for deep water waves, the wave phase celerity was known. Since the phase velocity is twice as big as the group velocity, a waiting time was needed after the wave maker started and before the carriage moved. This waiting time should be adjusted so that the centre of gravity of the model is located on a wave crest or on a wave trough.

Figure 9 shows the three different phases of a run: (1) zero carriage speed, the model is freely oscillating; (2) the carriage accelerates and the encounter frequency decreases; (3) the carriage speed is equal to the wave celerity, then the model is in surf-riding conditions.

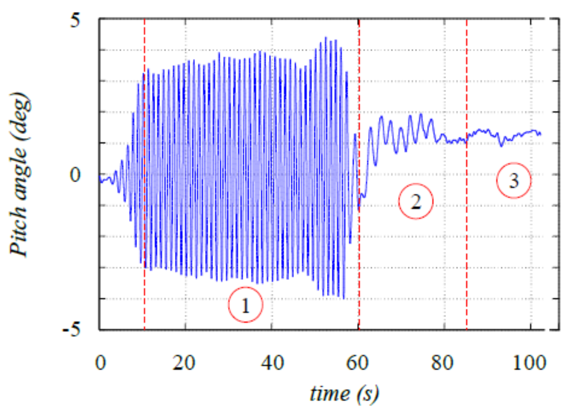

Fig. 9 - Pitch angle for $\lambda/L_{wl} = 1$ and $H/\lambda = 0.03$

Comparison between theoretical results and experimental results while the model was in surf-riding conditions is presented on figure 10.

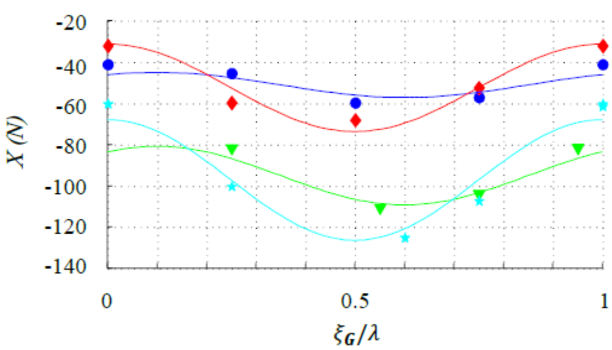

Fig. 10 - Straight towing in surf-riding conditions: surge force as a function of model position on the wave ($\xi_G/\lambda = 0$ at the wave trough; $\xi_G/\lambda = 0.5$ at the wave crest)

The legend used in the graph is as follow:

- ● *Experimental values for* $H/\lambda = 0.03$ *and* $\lambda/L_{wl} = 1$
- ♦ *Experimental values for* $H/\lambda = 0.05$ *and* $\lambda/L_{wl} = 1$
- ▼ *Experimental values for* $H/\lambda = 0.03$ *and* $\lambda/L_{wl} = 1.25$
- ★ *Experimental values for* $H/\lambda = 0.05$ *and* $\lambda/L_{wl} = 1.25$
- — *Mathematical model for* $H/\lambda = 0.03$ *and* $\lambda/L_{wl} = 1$
- — *Mathematical model for* $H/\lambda = 0.05$ *and* $\lambda/L_{wl} = 1$
- — *Mathematical model for* $H/\lambda = 0.03$ *and* $\lambda/L_{wl} = 1.25$
- — *Mathematical model for* $H/\lambda = 0.05$ *and* $\lambda/L_{wl} = 1.25$

While the ship is surfing near the wave trough, it appears that the measured resistance force is lower than at the wave crest. This phenomenon can be explained since in that position, the ship is in stationary conditions where she is pushed forward by the wave from the stern.

Since our model is relatively accurate for zero encounter frequency, further analysis has been done in order to distinguish 3 main modes of motion: the ship is overtaken by the wave, the ship is in stable surf-riding and the ship slowly overtakes the wave. This implies taking into account the effect of the encounter frequency ω_e into the mathematical model. The encounter frequency is calculated as follow, with V_φ the phase velocity of the wave and λ the wavelength:

$$\omega_e = 2\pi \frac{|V_\varphi - U_C|}{\lambda} \qquad (9)$$

Then, figure 11 shows that a good correlation is obtained in terms of mean value, amplitude and phase with the experimental results. Thus, the effect of non-linear functions $f_A(\omega_e)$, $f_{offset}(\omega_e)$ and $f_\varphi(\omega_e)$ is relevant when trying to simulate the ship's behaviour in following seas.

- The ship is overtaken by the wave:
  - ● *Experimental values for* $\omega_e = 2.2\ rad/s$
  - ♦ *Experimental values for* $\omega_e = 0.8\ rad/s$
  - ▼ *Experimental values for* $\omega_e = 0.3\ rad/s$
  - — *Mathematical model for* $\omega_e = 2.2\ rad/s$
  - — *Mathematical model for* $\omega_e = 0.8\ rad/s$

— *Mathematical model for* $\omega_e = 0.3\ rad/s$

- The ship is surfing the wave:
  - • *Experimental values for* $\omega_e = 0\ rad/s$
  - — *Mathematical model for* $\omega_e = 0\ rad/s$
- The ship overtakes by the wave:
  - ★ *Experimental values for* $\omega_e = 0.4\ rad/s$
  - — *Mathematical model for* $\omega_e = 0.4\ rad/s$

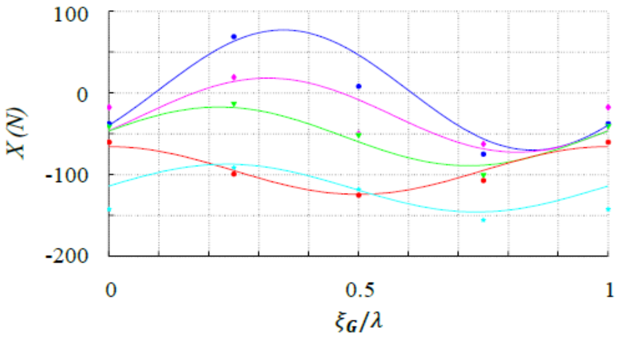

Fig. 11 - Straight towing in regular waves: surge force X plotted as function of ship position for $\lambda/L_{wl} = 1.25$ and $H/\lambda = 0.05$

7. Conclusions

Experimental and numerical studies are complementary when trying to understand a physical phenomenon since mathematical models are established from observations. There still are some recorded samples from the database that need to be post processed. For instance, pure sway and pure yaw tests while surfing regular waves need to be analyzed in order to give some quantified values to describe the broaching-to phenomenon.

However, a close correlation has been observed between the first results of our non-linear mathematical model and experiments. Once all measured data has been post-processed, and the hydrodynamic coefficients fully determined, it will be interesting to predict the ship's behaviour in following waves.

This work shows that captive model tests such as straight towing tests, oblique towing tests and several harmonic tests both in calm water and in following waves for different encounter frequencies and also at zero encounter frequency can be performed using the innovative measurement system we designed.

Future works will be done to validate our numerical-experimental *6 DOF* hybrid model by comparing the predicted behaviours with recorded behaviours from free-running model tests that will be carried out in the seakeeping and manoeuvring basin of the LHEEA. Then, quantitative values describing the surf-riding and broaching-to phenomena might be established and proposed to create new intact stability criteria.

Acknowledgments

This work is supported and funded with a PhD scholarship from DGA (Direction Générale de l'Armement) and the Pays de la Loire region.

Experiments have been performed thanks to the technical staff of the LHEEA basin.

References

[1] C. Wandji, P. Corrignan: Test Application of Second Generation IMO Intact Stability Criteria on a Large Sample of Ships, Proceedings of the 11th International Conference on the Stability of Ships and Ocean Vehicles, 2012.

[2] S. Hosseini, P. Carrica, F. Stern, N. Umeda, H. Hashimoto, S. Yanamura, A. Matsuda: CFD, system-based and EFD study of ship dynamic instability events: Surf-riding, periodic motion, and broaching, Ocean Engineering, Vol. 38, 2010, pp. 88-110.

[3] N. Umeda, A. Matsuda, M. Hamamoto, S. Suzuki: Stability assessment for intact ships in the light of model experiments, Journal of Marine Science and Technology, 1999, pp. 45-57.

[4] N. Umeda, H. Hashimoto, A. Matsuda: Broaching prediction in the light of an enhanced mathematical model, with higher-order terms

taken into account, Journal of Marine Science and Technology, 2003, pp. 145-155.

[5] H. Hashimoto, N. Umeda, A. Matsuda: Importance of several nonlinear factors on broaching prediction, Journal of Marine Science and Technology, 2004, pp. 80-93.

[6] Z. Ayaz, D. Vassalos, K.J. Spyrou: Manoeuvring behavior of ships in extreme astern seas, Ocean Engineering, 2005, pp. 2381-2434.

[7] R. Skejic, O.M. Faltinsen: A unified seakeeping and maneuvering analysis of ships in regular waves, Journal of Marine Science and Technology, JASNAOE, 2008.

[8] N. Umeda, S. Yamamura, A. Matsuda, A. Maki, H. Hashimoto: Model Experiments on Extreme Motions of a Wave-Piercing Tumblehome Vessel in Following and Quartering Waves, The Japan Society of Naval Architects and Ocean Engineers, 2008.

[9] S. Hosseini: CFD prediction of ship capsize: parametric rolling, broaching, surf-riding, and periodic motion, dissertation, University of Iowa, 2009.

[10] H. Hashimoto, N. Umeda, A. Matsuda: Broaching prediction of a wave-piercing tumblehome vessel with twin screws and twin rudders, Journal of Marine Science and Technology, 2011, pp. 448-461.

[11] Transportation Safety Board of Canada: Chavirement avec perte de vie du petit bateau de pêche Le Marsouin I, report number M09L0074, 2009.

[12] K. J. Spyrou: The nonlinear dynamics of ships in broaching, Marie Curie Fellowships Annals, Vol. 1, 2000.

[13] B. Horel, P.E. Guillerm, J.M. Rousset, B. Alessandrini: A method of immersed surface capture for broaching application, Proceedings of the ASME 2013 32nd International Conference on Ocean, Offshore and Arctic Engineering, 2013.

[14] D. Obreja, R. Nabergoj, L. Crudu, S. Pacuraru-Popoiu: Identification of hydrodynamic coefficients for manoeuvring simulation model of a fishing vessel, Ocean Engineering, Vol. 37, 2010, pp. 678-687.